Acoustic waveform inversion of ocean-bottom node seismic data

Sankar Sen and C.M. Varadarajan, ONGC, GEOPIC
Steve Syme, Weizhong Wang, and Yu Zhou, GeoTomo LLC;*

Keywords

Velocity Modeling, EAWI, AWI, Tomography, Ocean-Bottom Node

Summary

First arrival traveltime tomography has the ability to image complex near surface geology, but is unable to properly image a low velocity layer situated beneath a high velocity layer such as basalt. In this paper, we show that early arrival waveform inversion (EAWI) has the ability to see the low velocity layer underneath the basalt using ONGC ocean-bottom node (OBN) seismic data. As we have used only the PP data with constant density assumption, EAWI may be replaced by AWI, acoustic waveform inversion.

Introduction

In 2012, ONGC acquired approximately 800 km of 2D non-conventional Wide Angle Reflection/Refraction Profiling (WARRP) in the Kerala Konkan basin offshore India. Figure 1 shows the area of interest. The test line chosen for this study was 165 km long acquired with airgun source taken every 37.5 m. Thirty-three ocean bottom nodes were positioned 2 km apart, yielding data with offsets of more than 90 km. In addition to the seismic data, gravity and magnetic data was acquired. A low velocity zone (LVZ) was detected by using the combined seismic, gravity and magnetic data. The purpose of this study was to see if the seismic data alone could be used to detect the low velocity zone.

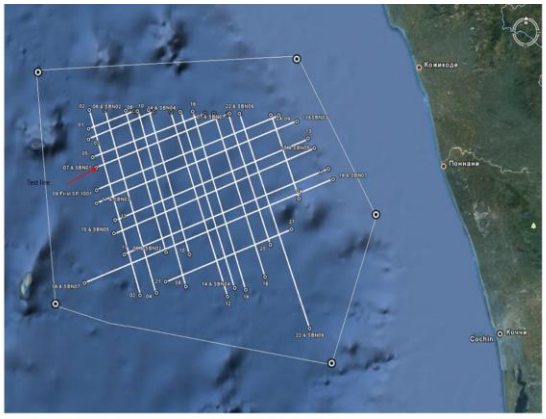

Figure 1: Area of interest showing 2D seismic.

Traveltime Tomography

First arrival traveltime tomography determines the near-surface velocities by examining the discrepancy between observed first arrival traveltimes and modeled traveltimes associated with an initial velocity-depth model. It perturbs the initial model parameters until the difference between the modeled and the picked traveltimes is minimized in the least-squares sense. We use the nonlinear traveltime tomography (Zhang and Toksoz, 1998) that accounts for the changes in the traveltime gradient to avoid the ill-posed inverse problem in solving the least-square equations. Iterate until the discrepancy between the modeled and the picked traveltimes, measured as the RMS errors in the inversion, has been reduced to a sufficiently small value comparable to the picking errors. The output is the final velocity-depth model for the near-surface, calculated model traveltimes, and the ray density associated with the final model.

For our test line, the geometry was checked, and the first breaks were picked through a combination of automatic picking plus some manual editing. An initial model was built and the nonlinear traveltime tomography was run. Although first breaks were picked out to offsets beyond 80km for some of the nodes, the shorter offsets had the most reliable picks. As such, only 10km of offsets were used for the final traveltime tomography model. Figure 2 shows the traveltime tomography result. Note that although there are higher velocities present in the velocity model, there is no evidence of a low velocity layer underneath the basalt layer.

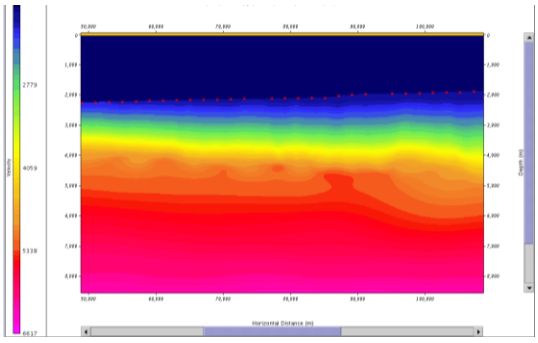

Figure 2: Result of nonlinear traveltime tomography

Acoustic waveform inversion of ocean-bottom node seismic data

Acoustic Waveform Inversion (AWI)

Full waveform inversion (Tarantola, 1984; Pratt, 1999) provides a more accurate solution than the traveltime tomography as it measures the discrepancy between observed and modeled seismic waveforms that have both amplitude and phase variations comparing with only single arrival traveltimes in the traveltime tomography.

Generally speaking, the traveltime tomography can resolve complex near-surface geology (Wang et al., 2012). However, the first arrival traveltime tomography may fail to image a low velocity layer below a high velocity top. This is because there may not be any rays refracted back from the low velocity hidden layer with the minimum traveltime.

To demonstrate this, we show the results of a model test with a low velocity layer underneath a high velocity layer. Figure 3 shows a synthetic model with a hidden layer. Figure 4 is its traveltime tomography result.

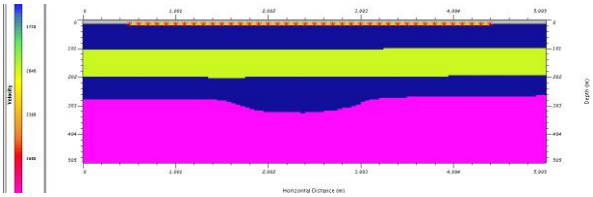

Figure 3: Model with a hidden layer.

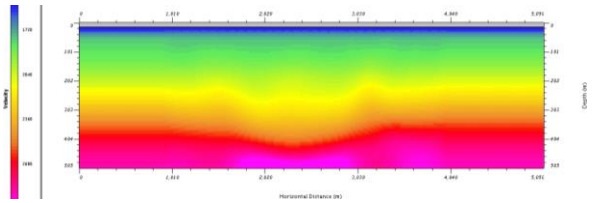

Figure 4: Traveltime solution of the model with the hidden layer.

Figure 5 shows early arrival AWI result for the hidden layer model. The low velocity layer can clearly be seen underneath the higher velocity, demonstrating the potential utility of AWI in such geologic settings.

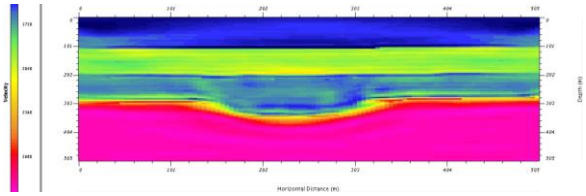

Figure 5: AWI result of the hidden layer model (Figure 3).

To run AWI on the OBN dataset, the data was muted above and below the early arrivals, and filtered with a low frequency bandpass to allow for easier matching of waveforms. We used the traveltime tomography result as the starting model.

Several iterations were run, and it can be seen that the resulting velocity model shows evidence of a low velocity layer underneath the higher velocity layer.

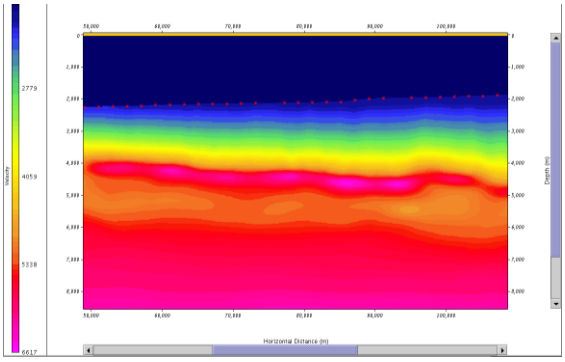

Figure 6: Early Arrival AWI solution showing a lower velocity layer underneath the basalt

One important QC of the validity of AWI result is to compare the synthetic waveform generated from the resulting model to the original input data. Figure 7 shows this waveform overlay at the start of the waveform tomography, while Figure 8 shows the waveform overlay after 10 iterations.

Acoustic waveform inversion of ocean-bottom node seismic data

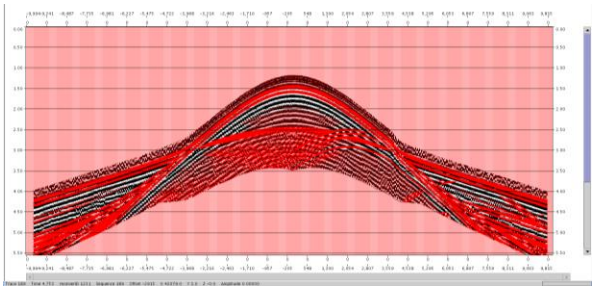

Figure 7: Shot record of synthetic (red) overlain on top of the preprocessed data input.

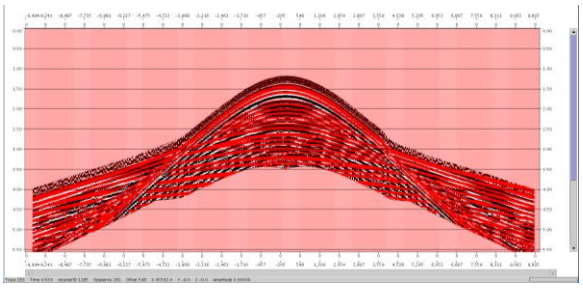

Figure 8: Waveform overlay after 10 iterations

Conclusions

For the long offset ocean-bottom node data, the traveltime tomography can do a reasonable job of constructing the true velocity model down to considerable depth. However, it fails to image the low velocity layer underneath the basalt. We have demonstrated, using both synthetics and real data, AWI has the ability to image a low velocity layer underneath the faster layer above.

References

Pratt, R. G., 1999, Seismic waveform inversion in the frequency domain, Part 1: Theory and verification in a physical scale model: Geophysics, **64**, 888-901

Tarantola, A., 1984, Inversion of seismic reflection data in the acoustic approximation: Geophysics, **49**, 1259-1266.

Wang, W., Jackson, J., and Syme, S., 2012, Near-surface solutions in seismic data processing: 9th Biennial International Conference & Exposition on Petroleum Geophysics, Hyderabad, India.

Zhang, J., and Toksoz, M. N., 1998, Nonlinear refraction traveltime tomography: Geophysics, **63**, 1726-1737.

Acknowledgements

Mr. Dibyendu Sar, ED (HOI), ONGC is thanked for providing necessary support to carry out the work. Special acknowledgement is due to GeoTomo LLC for providing TomoPlus software for the study. We express our sincere thanks to Kiran Pal, processing geophysicist of GEOPIC, ONGC for his technical assistance.

Views expressed in this study are exclusively of authors and do not reflect the view of the company.